Combustion iron distribution and deposition

Chao Luo,[1,3] N. Mahowald,[2,3] T. Bond,[4] P. Y. Chuang,[5] P. Artaxo,[6] R. Siefert,[7] Y. Chen,[8] and J. Schauer[9]

[1] Iron is hypothesized to be an important micronutrient for ocean biota, thus modulating carbon dioxide uptake by the ocean biological pump. Studies have assumed that atmospheric deposition of iron to the open ocean is predominantly from mineral aerosols. For the first time we model the source, transport, and deposition of iron from combustion sources. Iron is produced in small quantities during fossil fuel burning, incinerator use, and biomass burning. The sources of combustion iron are concentrated in the industrialized regions and biomass burning regions, largely in the tropics. Model results suggest that combustion iron can represent up to 50% of the total iron deposited, but over open ocean regions it is usually less than 5% of the total iron, with the highest values (<30%) close to the East Asian continent in the North Pacific. For ocean biogeochemistry the bioavailability of the iron is important, and this is often estimated by the fraction which is soluble (Fe(II)). Previous studies have argued that atmospheric processing of the relatively insoluble Fe(III) occurs to make it more soluble (Fe(II)). Modeled estimates of soluble iron amounts based solely on atmospheric processing as simulated here cannot match the variability in daily averaged in situ concentration measurements in Korea, which is located close to both combustion and dust sources. The best match to the observations is that there are substantial direct emissions of soluble iron from combustion processes. If we assume observed soluble Fe/black carbon ratios in Korea are representative of the whole globe, we obtain the result that deposition of soluble iron from combustion contributes 20–100% of the soluble iron deposition over many ocean regions. This implies that more work should be done refining the emissions and deposition of combustion sources of soluble iron globally.

1. Introduction

[2] Iron is a critical nutrient for organisms in the ocean because of its role in primary productivity and has been hypothesized to limit phytoplankton productivity in high-nitrate, low-chlorophyll (HNLC) ocean regions [e.g., *Martin et al.*, 1991]. Additionally, nitrogen-fixing organisms (diazotrophs) in the ocean are thought to have higher iron requirements than most ocean biota, and the high iron inputs to the North Atlantic may be related to the high nitrogen fixation in that ocean basin [*Capone et al.*, 1997; *Falkowski et al.*, 1998]. In the open ocean, new iron deposited from the atmosphere is thought to be important, and most previous studies have assumed that mineral aerosols are the source [e.g., *Fung et al.*, 2000]. On average, desert dust aerosols contain 3.5% iron [*Duce and Tindale*, 1991], primarily as relatively insoluble ferric iron (Fe(III)) in aluminosilicate form [e.g., *Zhu et al.*, 1997].

[3] The bioavailable fraction of iron is of primary importance to biogeochemistry, but it is not yet known what fraction is bioavailable. Previous studies [e.g., *Jickells and Spokes*, 2001; *Mahowald et al.*, 2005a, 2005b] assumed that soluble iron in the form of Fe(II) is bioavailable, and we use this assumption. In the source regions, iron in mineral aerosols it not very soluble [e.g., *Fung et al.*, 2000], but downwind observations show it is soluble [e.g., *Jickells and Spokes*, 2001]. It is thought that atmospheric processes, perhaps related to pollution, can convert iron to become more soluble in the atmosphere [e.g., *Jickells and Spokes*, 2001; *Mahowald et al.*, 2005a, 2005b; *Luo et al.*, 2005; *Fan*

[1]Department of Earth System Science, University of California, Irvine, California, USA.
[2]National Center for Atmospheric Research, Boulder, Colorado, USA.
[3]Now at Department of Earth and Atmospheric Sciences, Cornell University, Ithaca, New York, USA.
[4]Department of Civil and Environmental Engineering, University of Illinois at Urbana-Champaign, Urbana, Illinois, USA.
[5]Department of Earth Science, University of California, Santa Cruz, California, USA.
[6]Instituto de Fisica, Universidade de Sao Paulo, Sao Paolo, Brazil.
[7]Chemistry Department, U.S. Naval Academy, Annapolis, Maryland, USA.
[8]Department of Geological and Environmental Sciences, Stanford University, Stanford, California, USA.
[9]Department of Civil and Environmental Engineering, University of Wisconsin-Madison, Madison, Wisconsin, USA.

et al., 2006]. The specific mechanisms proposed vary from natural and anthropogenic organic acids, to nitrates and sulfates, and some emphasize the importance photooxidation in the presence of acids in cloud water [e.g., *Jickells and Spokes*, 2001; *Zuo and Hoigné*, 1992; *Zhuang et al.*, 1992] (see *Mahowald et al.* [2005a, 2005b] for a more thorough review). Some studies have emphasized the role of organic acids in complexing with the iron to maintain it as soluble [e.g., *Willey et al.*, 2004]. Although previous papers have mentioned the possibility of combustion sources of soluble iron [e.g., *Siefert et al.*, 1997; *Chen and Siefert*, 2004], one recent paper has argued that soluble iron comes predominately from combustion sources based on an observed high correlation between soluble iron and black carbon (from combustion) at Cheju, Korea [*Chuang et al.*, 2005]. Another study highlighted the possibility that biomass burning may be an important source of new iron to the ocean [*Guieu et al.*, 2005], and a very new paper also argues for a combustion source of soluble iron to the waters near Bermuda [*Sedwick et al.*, 2007]. Here for the first time we model the sources, transport, and deposition of iron from combustion sources to evaluate their importance. In order to determine whether iron from combustion is potentially important, we modeled the emission, transport, and deposition of iron, and the estimated emissions values are on the high end.

[4] For this study we will focus on understanding the soluble iron fraction observed at Cheju, Korea [*Chuang et al.*, 2005], as well as globally. This data represents a new set of observations, much closer to both dust and combustion sources than most of the observations available. We will test several hypotheses for the sources of observed soluble iron at Cheju using the model: atmospheric processing of dust particles, atmospheric processing of combustion iron, direct emissions of soluble iron from dust, and direct emissions of soluble iron from combustion processes. From these results we will estimate whether combustion sources of total iron or soluble iron can be neglected, as previously assumed [e.g., *Jickells and Spokes*, 2001; *Mahowald et al.*, 2005a, 2005b]. For this study we will build from our previous study, which looked at several different mechanisms for the conversion of iron to soluble iron and use the one which best matched the observations [*Luo et al.*, 2005].

[5] Our goals for this paper are to (1) estimate for the first time the total emissions of iron from combustion processes, (2) determine whether the correlations by *Chuang et al.* [2005] can be explained using a model including transport and chemistry phenomenon, (3) estimate particular regions where combustion iron may be important, and (4) provide soluble iron deposition maps for global ocean biogeochemistry models.

[6] This paper is organized in four sections. Section 2 describes the methodology, including a description of the model and observations used in the study. Section 3 presents the results, and section 4 contains a summary and discussion.

2. Methodology

[7] The chemical transport model used to simulate iron is the Model of Atmospheric Transport and Chemistry

(MATCH, version 4.2) [*Rasch et al.*, 1997], driven by National Center for Environmental Prediction/National Center for Atmospheric Research (NCEP/NCAR) reanalysis data set [*Kistler et al.*, 2001; *Mahowald et al.*, 1997]. The horizontal resolution of the model is T62 ($\sim$1.9 $\times$ 1.9 degree) and 28 vertical levels from surface to 10 mb.

[8] The model simulates sources, simple chemistry, and deposition of sulfur aerosols, carbonaceous aerosols, and sea salt aerosols [*Barth et al.*, 2000; *Rasch et al.*, 2000]. Emissions of sulfur species in the model include anthropogenic emissions of SO_2 and SO_4 and oceanic emissions of dimethyl sulfide (DMS). Anthropogenic emissions of SO_2 were obtained from the Global Emissions Inventory Activity (GEIA) emission inventory [*Benkoviz et al.*, 1996], which is representative of 1995 emissions. Distributions of oxidant species (e.g., OH, H_2O_2, and O_3) come from climatologies [*Rasch et al.*, 2000]. Black and organic carbon aerosols are modeled following *Rasch et al.* [2001] and *Collins et al.* [2001] and are emitted as hydrophobic aerosols. With a 1.2-d e-folding timescale, they are converted to hydrophilic aerosols, subject to wet deposition. Both hydrophobic and hydrophilic aerosols are subject to dry deposition processes. We include more details about the simulation of the dust and other iron containing aerosols below. Comparisons with observations for dust used correct day. For the combustion the results discussed below are the average of 1-year simulation from 1 January 2001 to 31 December 2001, with one additional month of spin-up not used for analysis. Comparisons with observations made during that year use the correct day. Comparisons with observations for other years use the appropriate monthly average. There are extensive comparisons of the dust simulations described here in the literature [e.g., *Luo et al.*, 2003; *Mahowald et al.*, 2002; *Hand et al.*, 2004; *Luo et al.*, 2005], but fewer comparisons for the sulfate and black carbon (BC) simulations: Therefore the online supplement contains figures (Figures S1–S4) which demonstrate that the model is doing a good job simulating these compounds at observational sites globally.[1]

[9] The modeling cases described below are summarized in Table 1. The different modeling cases can be linearly added together to simulate the potentially more realistic case that there are multiple sources of total and soluble iron.

2.1. Modeling of Total Iron
2.1.1. Mineral Aerosol Sources

[10] For the simulation of mineral aerosols or dust we use the Dust Entrainment and Deposition model [*Zender et al.*, 2003] within MATCH driven by NCEP winds. This combination has been extensively compared to observational data in previous studies [*Mahowald et al.*, 2002; *Luo et al.*, 2003; *Hand et al.*, 2004; *Luo et al.*, 2005]. This dust source parameterization is based on wind tunnel studies (see *Zender et al.* [2003] for a complete description). In order to include the effects of vegetation and varying soil erodibility this model includes the preferential source description of *Ginoux et al.* [2001]. Both dry deposition and wet

Table 1. Model Case Names

Case Name	Constituent Modeled
FE_DUST	total iron from dust
FE_ANTHRO	total iron from land use dust source
FE_COMB	total iron from combustion
SOLFE_DUST_AP	soluble iron from dust, due to atmospheric processing
SOLFE_COMB_AP	soluble iron from combustion, due to atmospheric processing
SOLFE_DUST_EM	soluble iron from dust, from emissions
SOLFE_COMB_EM	soluble iron from combustion, from emissions
SOLFE_COMB_BC	soluble iron from combustion, based on black carbon (BC)

deposition are included as loss processes for all aerosols [*Rasch et al.*, 2000]. Dry depositional processes for dust aerosol are simulated following *Seinfeld and Pandis* [1996] and include turbulent deposition and gravitational settling, with the latter dominating for large particles. We chose a globally constant particle size distribution at the sources, but allow four size bins to separately be transported and evolve [*Mahowald et al.*, 2002; *Luo et al.*, 2003; *Zender et al.*, 2003]; the mass source fractions are 0.1 for the class 0.1– 1 μm and 0.3 for the classes 1–2.5, 2.5–5.0, and 5.0– 10 μm, where the sizes are diameters of the particle. Within each bin we assume lognormal distributions in aerosol sizes [*Zender et al.*, 2003]. This case is the DUST model case in Table 1.

[11] In addition to the "natural sources" modeled here, we conduct one sensitivity study, where we include a proposed anthropogenic dust source from *Chin et al.* [2003]. They proposed a source in China from human land use, and we include this source as a preferential source area in our simulation as a sensitivity test, calling this case FE_ANTHRO.

[12] We assume that dust is 3.5% iron [*Duce and Tindale*, 1991]. Assuming a spatially heterogeneous fraction of iron in the source areas only changes our iron deposition amounts by less than 50% [*Hand et al.*, 2004; *Mahowald et al.*, 2005a, 2005b], smaller than other uncertainties in this study.

2.1.2. Total Iron Emissions From Combustion

[13] Emissions of iron from combustion sources were calculated using the Speciated Particulate Emission Wizard (SPEW). This program calculates emissions by combining fuel consumption data given by the *International Energy Agency* [1998a, 1998b], tabulated emission factors, and estimated technology prevalence. *Bond et al.* [2004] described this program and the resulting inventories of black and organic carbon. Information added to SPEW for this study included fraction of aerosol with diameters above 1 μm (supermicron), removal efficiencies for supermicron aerosols by particulate controls, and fractions of Fe in submicron and supermicron aerosols.

[14] Percentages of Fe found in fine and coarse particulate matter are given in Table 2. Our goal in this paper is to assess whether combustion sources of iron are potentially important, so we estimate Fe emissions that are on the high end of a reasonable range. For the most important process, coal burning, the lower end estimates of iron emissions

would be a factor or two lower, but for some processes it could be an order of magnitude. Thus our estimates are probably within a factor or two for the total emissions of iron. These values were multiplied by mass of fine and coarse particulate matter emissions calculated by SPEW. For coal combustion in stokers or residential applications, fine particulate matter is primarily carbonaceous. We assumed that mineral matter made up all material that was not black carbon, organic carbon, or hydrogen and oxygen associated with the carbon. We then multiplied the mineral matter emission rate by the fractions in Table 2. Coarse particles from coal combustion are usually mineral matter [*Flagan and Friedlander*, 1978], and we applied the elemental fractions to the entire coarse-mode emission.

[15] Most of the iron (>75%) comes from coal combustion from either power plants or industry in both the fine and coarse modes with the remainder coming from residential heating (coal or biofuel). About 85% of the emissions of iron are simulated here to be in the coarse mode. Because coal burning is so important, especially for coarse-mode particles, more accurate estimates of anthropogenic contribution will require using regionally specific values of ash content. Vehicle emissions of iron are negligible. Control efficiencies, based on technology in each region, were regionally specific, but these could be refined with additional information in the future.

[16] The iron emission rates were found to be very sensitive to assumed control technology, which was poorly known. In SPEW, differences in combustion practice among world regions are handled by specifying the fraction of fuel burned in different technologies. Each specified technology is a combination of combustion type and end-of-pipe emission controls. The fraction of particulate matter removed by control devices, and the division between different technologies, are major uncertainties in the amount of mineral matter emitted. Calculated uncertainties in mineral matter emissions and, correspondingly, in combustion iron are about a factor of 4–5 for both fine and coarse particles. The uncertainties of largest magnitude are in emissions from coal combustion. Total mineral matter emissions are actually more uncertain than those of black carbon, because all coal combustion produces mineral matter emissions, while only small combustors are thought to produce black carbon. Thus lack of knowledge about coal combustion practice has a much greater effect on mineral matter emissions. Uncertainties in Asia are of greater absolute magnitude than those in better characterized world regions, but the relative values are similar. Emissions from uncontrolled or small installations are responsible for this similarity. Although those installations may comprise a smaller fraction of the fuel combusted in North America and Europe, their contribution to the regional total is significant, and lack of characterization leads to large uncertainty.

[17] For the iron combustion sources we assume that the submicron iron is transported similar to black carbon in the model, but the coarse mode iron is distributed into the dust size bins in the following fashion: 20% in bin 2, 30% in bin 3, and 50% in bin 4, on the basis of observational estimates of the size distribution of particles emitted from coal combustion [*McElroy et al.*, 1981; *Linak et al.*, 2000].

Table 2. Emission Factors for Iron in Industrial Combustion Sources (Percent by Mass)

Source	Citation	Fine	Coarse	Notes
	Fossil Fuels			
Coal: power/industrial	*Olmez et al.* [1988]	7.6%	8.1%	
	Smith et al. [1979]	4.5%	-	
	Mamane et al. [1986]	7.5%	9.4%	
value used		*7.5%*	*9%*	
Coal: residential	T. C. Bond (unpublished data, 2005)	0.1%	0.1%	
Coal briquettes	T. C. Bond (unpublished data, 2005)	1.6%	-	
Oil boiler	*Olmez et al.* [1988]	1.6%	2.95%	
	Mamane et al. [1986]	1.7%	-	
	Hildemann et al. [1991]	0.13%	-	
value used		*1.6%*	*3%*	
Gasoline engines	*Kleeman et al.* [2000]	-	-	a
Diesel engines	*Kleeman et al.* [2000]	-	-	a
	Industrial Processes			
Blast furnaces	*Mamuro et al.* [1979a]	16%	16%	b
Coking	*Mamuro et al.* [1979b]	0.6%	0.6%	b
	Biofuels			
Agricultural wastes	*Andreae and Merlet* [2001]	0.2%	-	
		-	-	
Wood	*Andreae and Merlet* [2001]	-	-	a
	T. C. Bond (unpublished data, 2005)	0.2%	-	
Animal waste	No data found			
Charcoal	No data found			
	Waste			
Incinerator	*Olmez et al.* [1988]	0.22%	1.7%	
	Biomass Burning			
Cerrado flaming fire	*Yamasoe et al.* [2000]	0.077%		
Cerrado smoldering fire	*Yamasoe et al.* [2000]	0.045%		
Tropical forest flaming fire	*Yamasoe et al.* [2000]	0.031%		
Tropical forest smoldering fire	*Yamasoe et al.* [2000]	0.048%		
Georgia prescribed burn	*Lee et al.* [2005]	0.8%		
Typical tropical fire	Here and *Fuzzi et al.* [2007]	0.15%	3.4%	
	value used (Fe/BC ratio)	0.02	1.4	c

[a]Fe not reported; we assumed that it would have been if significant.
[b]No size-fractionated data available.
[c]Units are different on this line (Fe/BC ratio instead of % mass).

Sensitivity studies show that the results are not qualitatively affected by the exact distribution in the coarse size bins (not shown).

[18] As shown in Table 2, there are limited emission estimates of Fe from biomass burning [*Yamasoe et al.*, 2000]. The literature suggests there may be some iron associated with dust particles being entrained in large biomass burning fires [e.g., *Gaudichet et al.*, 1995; *Guieu et al.*, 2005], as well as iron that was in the plant material being entrained into the atmosphere during burning. In addition to the estimates from *Yamasoe et al.* [2000], we have available additional observations in the Amazon that we will use to estimate the iron emissions from biomass burning. We will focus on measurements made at Rondônia (11°S, 62°W) [*Fuzzi et al.*, 2007] because this region is 2–3 d downwind of the biomass burning regions and thus should contain aerosols representative of what will be deposited over ocean regions.

[19] The aerosol sampling and analysis techniques were described in some detail by *Fuzzi et al.* [2007] and are only briefly described here. Aerosol samples were collected for the fine- and coarse-mode fraction separately using stacked filter units and high-volume dichotomous samplers. Ele-

mental analysis was conducted using particle-induced X-ray emission analysis. Black carbon concentrations were obtained by an evolved gas analysis [*Novakov et al.*, 1997]. Ninety fine and ninety-one coarse daily averaged values were used for this analysis.

[20] In order to obtain an estimate of the iron emissions from biomass burning. we correlate iron with black carbon, whose main source is biomass burning. The correlation coefficients (R) are 0.78 and 0.68 for the fine and coarse fraction, respectively, and these values are statistically significant at the 99% level. The slope of the Fe to BC relationships (shown in Figure 1) is 0.02 for fine-mode and 1.4 for coarse-mode aerosols. The spatial and temporal extent of biomass burning is modeled based on the work of *van der Werf et al.* [2003], which uses satellite data and a terrestrial carbon model to estimate carbon and aerosol releases from biomass burning during specific years. For this study we use the average monthly mean over 1997–2004. Fine-mode iron from combustion is modeled similar to black carbon in the model, while coarse-mode iron is modeled similar to the largest two size bins of dust (described above). The sum of the biomass burning and
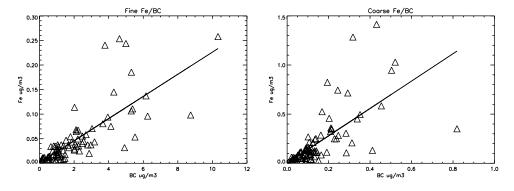
Figure 1. Iron verus black carbon for the observations in the Amazon [from *Artaxo and Maenhant*, 1990; *Mahowald et al.*, 2005a, 2005b] for fine-mode (a) and coarse-mode (b) aerosols.

industrial sources of iron described in this section is modeled in the FE_COMB cases (Table 1).

2.2. Soluble Iron Modeling

[21] In this paper, we consider two different mechanisms for soluble iron from each of our two source types (dust or combustion): atmospheric processing and direct emission. These cases are indicated in Table 1 as SOLFE cases.

2.2.1. Atmospheric Processing Production of Soluble Iron

[22] In this paper, we simulate the processing of the atmospheric combustion iron to become more soluble using the Hematite hypothesis approach (HP case from *Luo et al.* [2005] as described by *Luo et al.* [2005] following the ideas of *Meskhidze et al.* [2003], and including the impact of clouds as well (case CP + HP from *Luo et al.* [2005]). Notice that this case performed better than the cases we examined using organic acids or other mechanisms [*Luo et al.*, 2005]. For the CP case we modify the rate coefficients from *Luo et al.* [2005] by reducing them by a factor of 10 to better match the cruise observations of soluble iron: Previously, our CP case had too much soluble iron compared to observations. This is similar to the ideas of *Fan et al.* [2006], but included in a much simpler way. In the work of *Luo et al.* [2005] we look at several different processes that might be responsible for atmospheric conversion of iron from insoluble to soluble form, and this case is one of the best in comparisons with observations in our previous study [*Luo et al.*, 2005]. Below we describe the CP + HP processes.

[23] We estimate the effects of cloud processing on soluble iron by assuming that the conversion to soluble iron occurs once insoluble iron comes into contact with a cloud [*Siefert et al.*, 1997; *Saydam and Senyuva*, 2002]. This case assumes that the clouds are always sufficiently acidic to process the iron to become more soluble, and the important process to model is whether the iron is in a cloud or not. The decay rate (K_{cld}) was computed with equation (1)

$$K_{cld}(i,j) = \frac{C(i,j)}{C_{avg}} \bigg/ \tau_{OBS} \qquad (1)$$

where C(i, j) represents the fraction of a grid box that is cloudy in the model at each level, and C_{avg} is the average fraction in the tropics around 10°N (C_{avg} = 0.05). (= 0.05). We picked the tropical cloud fraction because that is the area of most of the dust transport. $\hat{O}_{ob}s$ is estimated from observations different transport times downwind from the sources [*Hand et al.*, 2004]. For this study we reduce the decay rate by a factor of 10 from that by *Hand et al.* [2004] or *Luo et al.* [2005] to better match the cruise observations of soluble iron.

[24] *Meskhidze et al.* [2003] argue, using an aerosol equilibrium box model, that the acidity of the aerosol is critical to the conversion of Fe(III) to Fe(II), and that anthropogenic sulfate plays an important role in modulating acidity in the Pacific. In order to test their hypothesis in a global model, we simplify the reactions considerably, looking only at hematite in dust as a source of iron. Following their hypothesis, we implement a mass balance equation for dissolved Fe (equation 2):

$$\frac{d[FE(II)]}{dt} = W(Fe_{hem}) \cdot R_{hem} \cdot [dust] \qquad (2)$$

where (Fe(II)) is the soluble concentration, (Dust) is the mass fraction of the mineral aerosol (g/g), WFe_{hem} is the number of moles of Fe in a mole of hematite (2); and R_{hem} is the hematite dissolution rate (moles of dissolved hematite (g of dust)$^{-1}$ s^{-1}). For R_{hem} we adopt the formulation of *Lasaga et al.* [1994], similar to *Meskhidze et al.* [2003] (equation (3)):

$$R_{hem} = K_r(T) \cdot a(H^+)^m \cdot f(\Delta G_r) A_{hem} W_{hem} \qquad (3)$$

where K_r is the temperature (T) dependent reaction coefficient (moles dissolved m^{-2} of mineral s^{-1}), $a(H^+)$ is the H$^+$ activity, m is an empirical parameter, f is a function of Gibbs free energy (ΔG_r), and accounts for the variation of the rate with deviation from equilibrium [*Cama et al.*, 1999], A_i is the specific surface area of mineral aerosols in units of m^2 g^{-1}, and W_i is the weight fraction of the mineral in dust in units of g of mineral (g of dust)$^{-1}$. The equation f(ΔG_r) = 1 was used in our simulation. Values for hematite are m = 0.5; Ai = 100 (m^2/g); and Wi = 5%; while reaction coefficient K_r depends on the total amount of the hematite
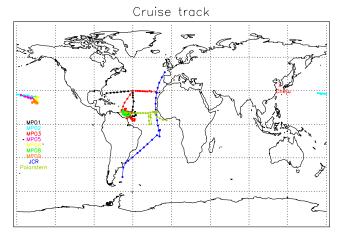
Figure 2. Cruise tracks for soluble and total iron data shown in this study. Data is taken from *Baker et al.* [2003, 2006], *Chen and Siefert* [2003, 2004], and *Chen* [2004], as described in more detail in the text.

already dissolved, following *Meskhidze et al.* [2003], *Azuma and Kametani* [1964], *Blesa et al.* [1994], *Cornell and Schwertmann* [1996], *Zinder et al.* [1986], and *Skopp* [2000]:

Stage I(0 to 0.8% of total oxide dissolved)

$$K_r = 4.4 \times 10^{-12} \exp\left(9.2 \times 10^3 (1/298 - 1/T)\right)$$

Stage II(0.8 to 40% of total oxide dissolved)

$$K_r = 1.8 \times 10^{-11} \exp\left(9.2 \times 10^3 (1/298 - 1/T)\right)$$

Stage III(40 to 100% of total oxide dissolved)

$$K_r = 3.5 \times 10^{-12} \exp\left(9.2 \times 10^3 (1/298 - 1/T)\right) \qquad (4)$$

[25] For the pH value calculation we simply set pH = 7.5 when concentration of Ca is larger than the concentration of SO_4, and pH = 2 when concentration of SO_4 is larger than the concentration of Ca, and assume that 6% of dust is soluble Ca. K_r was calculated depending on the amount of hematite dissolved and temperature. By assuming all the iron is in hematite (while it may also be in other forms, such as alumisilicates) we may be overestimating the conversion of iron to soluble iron.

[26] The case where soluble iron is determined from this mechanism is called the AP (atmospheric processing) case in Table 1 and is applied to both dust and combustion sources in the model simulations.

2.2.2. Direct Emission of Soluble Iron

[27] In addition, we model cases where the soluble iron is assumed to be determined at emission and does not evolve with time and use soluble iron estimates from the *Chuang et al.* [2005] data in order to estimate these solubilities. We do this in two different ways for combustion sources. For both combustion and dust sources we use the observations to estimate a soluble fraction emitted. We also assume a simple ratio between iron and BC, on the basis of the observations, for a second combustion case.

[28] The data at Cheju and data collected closer to the dust source in Asia (Dunhuang) are consistent with a different soluble iron fraction in dust than in combustion sources. Average soluble Fe/total Fe at Dunhuang in China is 0.45%, ranging from 0.05% to 1%. We use 0.45% soluble iron for the FE_DUST total iron case in order to generate the SOLFE_DUST_EM (emission) model case in Table 1 for all bin sizes.

[29] In order to estimate the solubility of the combustion source, we use the data at Cheju, but only for non-dust-dominated days. We eliminate the obvious dust event days, and remove the next 25% to eliminate combined dust and pollution events and average the highest 75 percentile of the soluble iron data (to get rid of low values from dust events), and obtain a soluble iron percentage from combustion sources of 4.0%, almost $10\times$ higher than the average soluble iron percentage close to the dust sources (0.45%). This is similar to the high solubilities deduced from nondust sources by *Baker et al.* [2006]. We multiply this solubility by the iron in the combustion source (FE_COMB) to get the soluble iron case SOLFE_COMB_EM in Table 1. Notice, here we are assuming that Fe(II) would be stable in the atmosphere, which may not be a good assumption.

[30] Finally, because of the high correlation between black carbon and soluble iron in the observations (0.4 as reported here from the Cheju data), we use the observed slope between soluble iron and black carbon, and model black carbon distributions to deduce soluble iron distributions. This slope is 0.02 soluble iron/black carbon. We thus model the black carbon in the model and use that concentration or deposition multiplied by 0.02 in order to estimate the soluble iron in this case, called SOLFE_COMB_BC in Table 1.

2.3. Total and Soluble Iron Measurements

[31] In order to assess whether the modeled iron distributions are reasonable, we compare to different previously published sets of measurements. One set comes from the study of *Chuang et al.* [2005] and shows soluble iron, total iron, and other constituents taken at the Dunhuang and Cheju site during Ace Asia. This measurement definition of soluble iron includes all iron that can pass through a 0.2 micron filter. This will include some colloidal iron, which is likely to be bioavailable to phytoplankton [e.g., *Chen et al.*, 2003; *Nishioka et al.*, 2005; *Parekh et al.*, 2004].

[32] The second set is a compilation of iron solubility data taken from eight cruises compared to model results by *Luo et al.* [2005] and is described in more detail there. Figure 2 shows the location of the different cruises used here to compare against data. Table 3 shows the different cruises used in this study and the appropriate reference for more details on the measurement method.

[33] For most of our analysis we use the consistent measurements taken during 2001–2003 of Fe(II) [*Chen and Siefert*, 2003, 2004]. However, the Southern Ocean cruises of *Baker et al.* [2003] tended to show the most disparity between observations and different model cases [*Luo et al.*, 2005]. Therefore we use a crude method to convert from "labile" iron measured by *Baker et al.* [2003, 2006] to a value equivalent to Fe(II) by multiplying by 0.5, as found in comparisons of data in the *Luo et al.* [2005]

LUO ET AL.: COMBUSTION IRON

Table 3. Soluble and Total Fe Cruise Measurements

Cruise Name	Location	Citation
MP01	North Atlantic	*Chen and Siefert* [2004]
MP02	North Pacific	*Chen and Siefert* [2004]
MP03	North Atlantic	*Chen and Siefert* [2003]
MP05	North Pacific	*Chen* [2004]
MP06	North Pacific	*Chen* [2004]
MP08	equatorial Atlantic	*Chen* [2004]
MP09	North Pacific	*Chen* [2004]
JCR	Atlantic transect	*Baker et al.* [2003]
Polarstern	Atlantic transect	*Baker et al.* [2006]

study. This will allow us to include the *Baker et al.* [2003, 2006] measurements in a semiquantitative way.

3. Results and Discussion

[34] Combustion and mineral aerosol sources of iron have different geographic distributions, reflecting their different sources (Figure 3). Combustion iron sources from industri-

alized processes are concentrated in East Asia, Europe, and the east coast of North America, while biomass burning sources of iron occur largely in the tropical regions. Mineral iron sources are predominantly from the arid subtropics, such as north Africa, the Arabian Peninsula, Australia, and East Asia. Total iron emissions from mineral dust are 55 Tg/a, while iron from biomass burning and other combustion sources is around 1.07 and 0.66 Tg/a, respectively. Thus in terms of source and deposition, the mineral aerosols dominate combustion sources of iron by a factor above 30, on the basis of the assumptions used here. As discussed in section 2, the emissions of total iron from combustion are quite uncertain, and if it proves important, these emission estimates should be refined.

[35] Figure 4 shows the distribution of total iron deposition from combustion (FE_COMB) and mineral aerosol (FE_DUST) sources and the percentage of deposition from combustion. The lifetime of combustion iron is 3.24 d which is smaller than dust iron lifetime of 5.26 d. This is partly because of the different size distribution for combus-
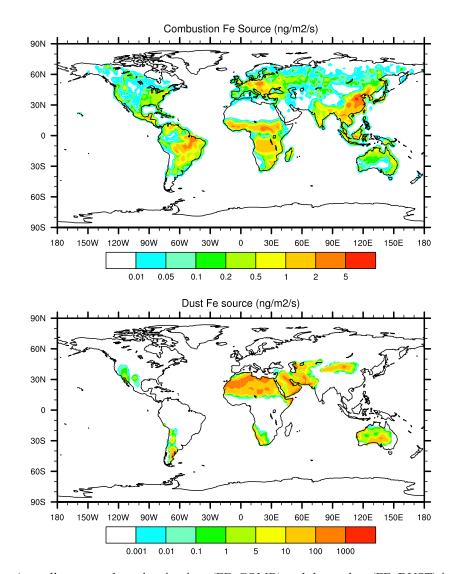

Figure 3. Annually averaged combustion iron (FE_COMB) and desert dust (FE_DUST) iron sources.

Combustion Fe Deposition (ng/m2/s)

Dust Fe deposition (ng/m2/s)

Ratio of Combustion Fe deposition/Total Fe Deposition (%)
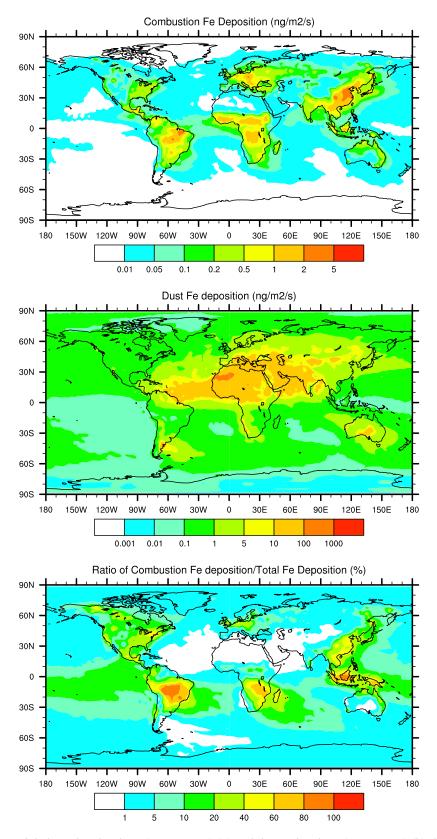
Figure 4.   Modeled combustion iron (FE_COMB) (a) and desert dust iron (FE_DUST) (b) deposition to oceans, and the percentage of the total deposited iron which comes from combustion (FE_COMB)/ (FE_COMB + FE_DUST).
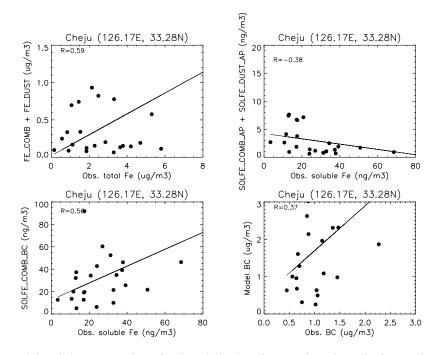
Figure 5. Model and data comparison for the Cheju data for March and April of 2001 for the cases of FE_COMB + FE_DUST compared to observed total iron (a); SOLFE_COMB_AP + SOLFE_DUST_AP compared to observed soluble iron (b); SOLFE_COMB_BC compared to observed soluble iron (c); and modeled BC vs. observed BC.

tion iron, but mostly because it is emitted in wetter regions. In broad areas surrounding source regions the combustion source of iron represents up to 50% of the iron deposition. Over the Pacific and Atlantic oceans, away from the coast, the combustion source tends to be less than 5% of the total deposition, with a fraction above 20% close to the Asian continent. Thus this analysis would suggest that for total iron deposition to the open oceans, combustion sources are not important.

[36] We start our discussion by comparing to the daily averaged values at Cheju, since these are the measurements which motivate this study. *Chuang et al.* [2005] argue that combustion sources of soluble iron may be important, on the basis of observed correlations between soluble iron and black carbon (0.4, statistically significant at the 95%), and the observed lack of correlation between soluble iron and total iron (−0.2, not statistically significant) at Cheju, Korea (33°N, 126°E) (see Table 4; these values are slightly different than those reported by *Chuang et al.* [2005], because of different data being included). At this station there is approximately one month of data (26 individual daily averages). Here we compare our model results to their observations (Figure 5 and Tables 4, 5, and 6). Our results suggest that the model has some ability to capture the day-to-day variability in pollution, at Cheju, since the R of total iron, sulfate, and black carbon in the model versus observations are 0.6, 0.3, and 0.4, respectively (for statistical significance, see Table 6). This ability to capture the daily averaged variability means that we are capturing episodic pollution events as they come over from the Asian mainland and is typical of correlations at stations that are well

captured by the model (e.g., for comparison, see daily averaged correlations of dust by *Mahowald et al.* [2002, 2003]). The ability to capture variability in total iron is not dependent on the inclusion of the combustion sources iron, since iron associated with dust dominates in the model simulations (Tables 5 and 6). The contribution of different sources of iron to the emissions and deposition to oceans is shown in Table 7.

[37] The model is not able to capture the absolute magnitude of the total iron reaching Cheju during April and is low by almost a factor of 7 (Figures 5 and 6). The model is biased low in general (Figure 5), and the failure of the model to capture the seasonal cycle in 2001 makes the bias even worse. The model is a factor of 3 lower in the annual average when the correct years are compared in the model versus observations (0.63 versus 0.21 μg/m3; see Figure 6). We explored whether fixable model errors could account for this discrepancy. *Chin et al.* [2003] hypothesized that there was an anthropogenic source of dust. Including this source in our model (FE_ANTHRO) does not improve the model's ability to capture either the seasonal cycle (Figure 6) or daily averaged variability in total iron (R = 0.15, not statistically significant, Table 6). We also explored whether the model was offsetting the transport of the dust slightly or

Table 4. Observed Correlation Coefficients (R) at Cheju[a]

	Total Fe	Soluble Fe	BC
Soluble Fe	−0.21	-	-
BC	**0.42**	**0.40**	-

[a]Bold results are significant at the 95% level.

Table 5. Modeled Correlation Coefficients (R) at Cheju[a]

	FE_COMB + FE_DUST	SOLFE_COMB_AP + SOLFE_COMB_AP	SOLFE_COMB_BC
FE_COMB	**0.86**	**0.45**	**0.51**
FE_DUST	**0.995**	**0.66**	0.00
BC	0.0	0.02	**1.0**
SOLFE_COMB_AP	**0.58**	**0.77**	**0.51**
SOLFE_DUST_AP	**0.58**	**0.995**	−0.05

[a]Bold results are significant at the 95% level.

not resolving the emissions from Korea (by one or two grid boxes), but this did not seem to resolve the April concentration problem. Downwind at the Midway and Hawaii stations, and closer to the source regions, the model captures the dust concentration and depositions [*Luo et al.*, 2003, Figures 4 and 5; *Hand et al.*, 2004, Table 2 and Figure 16; *Luo et al.*, 2005, Figure 5]. Thus we presume that there is a problem in the absolute magnitude of the dust reaching Cheju during April, but do not tune the annually averaged deposition to the Pacific basin.

[38] Next we look at the model's ability to capture the observed daily averaged variability at Cheju in soluble iron. In the observations, there are peaks in the measurements, as plumes of high dust and pollution events move across the sampling site, and these are clearly seen in the daily averaged observations. For the model simulations the suffix AP means that soluble iron comes about through atmospheric processing alone; the suffix EM means iron has a certain soluble fraction at emission and that this does not change during its atmospheric lifetime (see Table 1 and section 2 for more details). Comparisons of soluble iron between the observations and model-derived values based on atmospheric processing (SOLFE_COMB_AP + SOLFE_DUST_AP) show that the model is not able to capture the observed variability in the soluble iron using atmospheric processing (R = −0.4, Table 6). The model does not get sufficient soluble iron (SOLFE_COMB_AP + SOLFE_DUST_AP) reaching Cheju by a factor of 10, although this is consistent with too little total iron reaching the site. The modeled soluble iron from atmospheric processing (SOLFE_COMB_AP + SOLFE_DUST_AP) does not correlate with the modeled black carbon (R = 0.02, Table 5), as it does in the observations. This suggests that

atmospheric processing alone of soluble iron, as represented in our model, is not accurately capturing the relevant processes at this station over this limited time period.

[39] Cases SOLFE_COMB_EM and SOLFE_DUST_EM (where soluble iron amounts are determined at emission) are also unable to capture the variability in Cheju (Table 6). However, the modeled black carbon based soluble iron (SOLFE_COMB_BC) correlates at a moderate level with the observed soluble iron (R = 0.56, statistically significant at the 95% level) and gets approximately the right amount of black carbon (within 40% of the averaged value). This case would also have a high correlation between BC and soluble iron in the model (R = 1.0). We use a ratio of 0.02 soluble iron to BC in this case, based on observations at Cheju. We may be overestimating biomass burning sources of soluble iron using this method, since we deduced a total iron to black carbon ratio of 0.02 for the fine fraction from data in Brazil (section 2.1.2), and we are thus implying all the iron is soluble. However, it may also be that iron emitted during biomass burning is very soluble. As far as we know, the ratio of soluble to total iron for biomass burning emissions has not been directly measured. The iron that emitted from biomass burning was partially in the plant material burned (and partially in more insoluble soil particles entrained by the plume), and presumably was bioavailable at that point. We observe quite significant amounts of zinc in aerosols emitted by biomass burning, and this Zn appears in ratios that are similar to the ratios observed in plant composition. A similar pathway could be true for iron, with the Fe that was embedded in the plant being emitted as aerosol particles during biomass burning. This suggests that Fe from biomass burning may have a higher soluble ratio than Fe from soil dust. Of course, if much of the iron

Table 6. Model/Data Correlation Coefficients (R) at Cheju[a]

	Observed Total Fe	Observed Sol Fe	Observed BC
Model BC	−0.19	**0.56**	0.36
FE_COMB + FE_DUST	**0.60**	−0.28	**0.60**
FE_ANTHRO	0.15	0.16	0.41
FE_COMB	**0.42**	0.02	**0.71**
FE_DUST	**0.61**	−0.33	**0.57**
SOLFE_DUST_AP	0.22	−0.43	0.16
SOLFE_COMB_AP	−0.06	−0.05	0.32
SOLFE_DUST_EM	**0.61**	−0.33	**0.57**
SOLFE_COMB_EM	**0.42**	0.02	**0.71**
SOLFE_COMB_BC	−0.19	**0.56**	0.36
Scenario 1: SOLFE_COMB_AP + SOLFE_DUST_AP	0.20	−0.39	0.19
Scenario 2: SOLFE_COMB_BC + SOLFE_DUST_EM	−0.16	**0.51**	0.34
Scenario 3 (sum of 1 and 2)	−0.15	**0.50**	0.35

[a]Bold results are significant at the 95% level. The R for SOLFE_COMB_EM is the same as FE_COMB, since they have the same variability and only differ by a constant. Similarly, the R for SOLFE_DUST_EM are the same as FE_DUST, and the R for BC is the same as SOLFE_COMB_BC.

Table 7. Combustion and Dust Aerosol Budget[a]

	Dust, Fe	Industrial Combustion, Fe	Biomass Burning, Fe
Emission	54.76	0.663	1.07
Deposition to ocean	11.86	0.083	0.149

[a]Unit: Tg/a.

emitted from biomass burning is associated with the soil dust incorporated into the biomass burning plumes, than we would not expect higher solubility. This must be tested with observations.

[40] Although combustion iron does not appear to correlate well with soluble iron, as shown by the SOLFE_COMB_EM case, it is possible that only certain sources produce soluble iron, and this is not captured by our current emission modeling. Black carbon is indicative of incomplete combustion, which may occur in a reducing atmosphere; the same combustion conditions could produce soluble iron. One simple explanation could be that black carbon is indicative of incomplete combustion. Soluble iron (Fe(II)) could also be indicative of incomplete combustion, since Fe(II) is less oxidized than the less soluble Fe(III). Thus BC and Fe(II) may be correlated in the data because they have similar sources, and a different distribution of sources than total iron sources from combustion. This hypothesis needs further testing. In addition, the emissions from sources that have incomplete combustion are not well characterized, and thus our emission estimates are more uncertain for those cases.

[41] Finally, we can also assume that soluble iron is both emitted and atmospherically processed, thus giving us three scenarios to compare against observations (also summarized in Tables 6 and 7): scenario 1, atmospheric processing of insoluble iron produces soluble iron (SOLFE_COMB_AP + SOLFE_DUST_AP); scenario 2, soluble iron is emitted directly (SOLFE_COMB_BC + SOLFE_DUST_EM); and scenario 3, soluble iron is both emitted and atmospherically produced (SOLFE_COMB_AP + SOLFE_DUST_AP + SOLFE_COMB_BC + SOLFE_DUST_EM). Scenario 3 is the linear combination of scenarios 1 and 2. We have already shown that scenario 1 is inconsistent with the data

at Cheju using our model, so we include that for comparison only (Table 6).

[42] The total amount of soluble iron deposited to different ocean basins changes under different scenarios (Figure 7), and the inferred importance of combustion sources of iron changes from not very important (scenario 1), to over 50% and thus quite important (cases 2 and 3). In scenario 1 the importance of combustion is similar to what is seen in Figure 4, as expected. In scenario 2, over much of the ocean, over 50% of the soluble iron comes from combustion sources of iron. In scenario 3, over most of the oceans, soluble iron deposition has a 20% or more contribution from combustion sources of iron. This includes the potentially iron limited basins of the eastern equatorial Pacific and much of the south Atlantic and Indian oceans, although this is less true in the southernmost parts of the Southern Ocean. The globally averaged deposition of soluble iron is 0.41 and 0.018 Tg/a from the atmospheric processing of dust and combustion total iron, respectively (scenario 1; see Table 8). While the globally averaged total iron deposition is above 30 times larger for dust than combustion sources (FE_DUST versus FE_COMB), the globally averaged soluble iron deposition assuming atmospheric processing is around 20 times larger for dust than combustion (SOLFE_DUST_AP versus SOLFE_COMB_AP) (Table 8). This is potentially linked to the smaller particle sizes of combustion iron, the increase in processing because of the emissions of sulfur in the same location, or the higher cloud amounts along the deposition pathways (storm tracks versus desert regions). In scenario 2 the globally averaged deposition of soluble iron is 0.25 and 0.21 Tg/a from dust (SOLFE_DUST_EM) and combustion (SOLFE_COMB_BC) sources, respectively, and for case 3 it is 0.66 and 0.22 Tg/a for dust (SOLFE_DUST_AP + SOLFE_DUST_EM) and combustion (SOLFE_COMB_AP + SOLFE_COMB_BC) sources of soluble iron, respectively. So in all three scenarios considered here, dust sources of soluble iron dominate globally, but not in all regions, as seen in Figure 7 and Table 8.

[43] A compilation of total iron observations (from the cruise tracks shown in Figure 2) show that the model is able to simulate total iron over many orders of magnitude (Figure 8), no matter whether combustion sources are
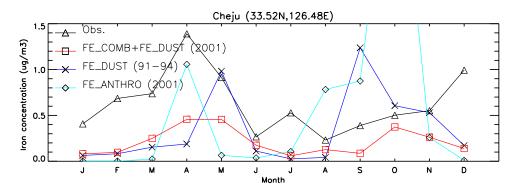

Figure 6. Monthly mean modeled and observed concentrations of iron at Cheju for different cases considered here.
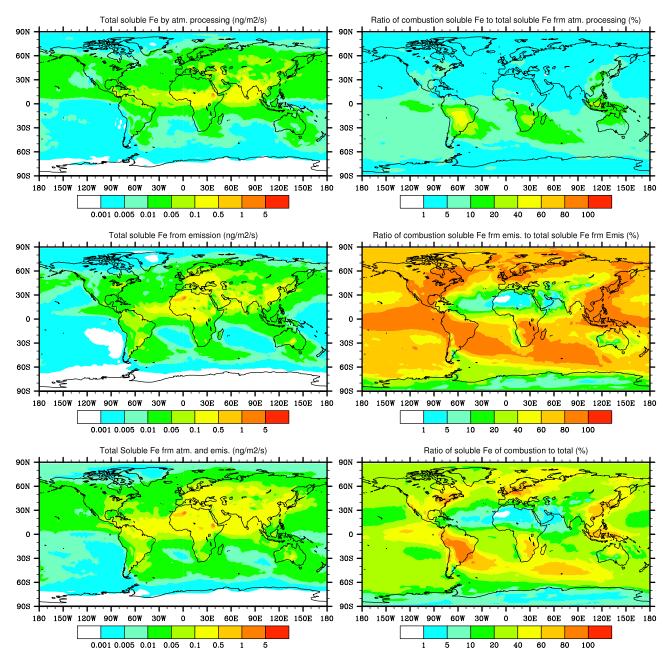
Figure 7. Modeled soluble iron deposition and fraction from combustion shown for scenario 1 (a and b) (SOLFE_COMB_AP + SOLFE_DUST_AP), scenario 2 (c and d) (SOLFE_COMB_BC + SOLFE_DUST_EM) and scenario 3 (e and f) (sum of scenario 1 and 2).

Table 8. Total and Soluble Iron in Each Scenario[a]

	Description	Soluble Iron Case Names	Total Iron Tg/a, Fraction From Combustion	Soluble Iron Tg/a, Fraction From Combustion
Scenario 1	atmospheric processing	SOLFE_COMB_AP + SOLFE_DUST_AP	56.5 (0.03)	0.43(0.04)
Scenario 2	emissions	SOLFE_COMB_BC + SOLFE_DUST_EM	560.5(0.03)	0.46 (0.46)
Scenario 3	atmospheric processing plus emissions	SOLFE_COMB_AP + SOLFE_DUST_AP + SOLFE_COMB_BC + SOLFE_DUST_EM	560.5(0.03)	0.89 (0.26)

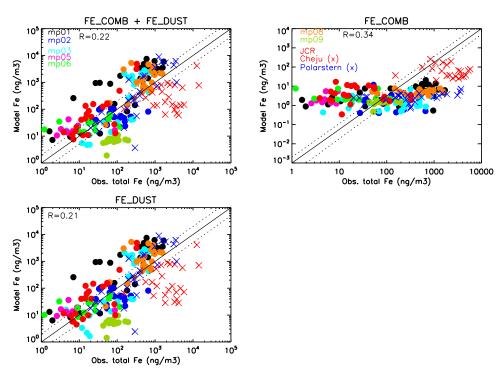[a]In the final two columns the fraction coming from combustion is in parentheses.

Figure 8. Comparisons of total iron concentrations for the different model cases for the cruises shown in Figure 2, FE_COMB + FE_DUST (a); FE_COMB (b); FE_DUST (c).

included or not. This is consistent with the model's ability to capture dust distributions globally [e.g., *Luo et al.*, 2003; *Hand et al.*, 2004; *Luo et al.*, 2005]. For soluble iron it is not really possible to determine which of the scenario's cases best match the limited observations (Figure 9): None of the scenarios presented here do a particularly good job of capturing spatial variability (R = ~0.2 for all cases), similar to previous studies [*Luo et al.*, 2005; *Fan et al.*, 2006]. The way we have modeled them here, scenario 2 is too low compared to observations (Figure 9), but scenarios 1 or 3 fit the cruise data fairly well; however, this is quite sensitive to our assumptions. However, the Cheju data is inconsistent with scenario 1 in our model. Thus scenario 3 is consistent with existing cruise data (Figures 8 and 9) and the station data at Cheju (Figure 5), although scenario 2 could be correct as well.

[44] *Baker and Jickells* [2006] show that there is an inverse relationship between iron solubility and the size of particles. Unfortunately, this observation does not help us discriminate between the processes considered here and understand whether combustion sources of iron are important. Smaller particles have a longer residence time, and therefore are more processed, and have a higher solubility as seen by *Hand et al.* [2004]. However, smaller dust particles could also be more soluble, because of differences in mineralogy [e.g., *Claquin et al.*, 1999], and combustion particles will tend to be smaller than dust particles, and be more soluble.

[45] If, indeed, combustion sources of soluble iron are important, this implies large changes in soluble iron distributions since preindustrial times. We explore this by assuming that 90% of the combustion in the model did not occur during the preindustrial climate (Figure 10) (without changing the climate forcing the simulation), and we use both scenarios 2 and 3 for this change. Figure 10 suggests a large perturbation to important regions of the ocean from the combustion source of soluble iron in the current climate relative to the preindustrial climate, if scenario 2 or 3 is true. In the case of scenario 2, over most of the oceans, deposition of soluble iron has doubled since preindustrial times, while in scenario 3, deposition of soluble iron has increased by 20% over much of the oceans, and by 50% over the eastern equatorial Pacific, southern Atlantic, and Indian oceans.

4. Summary and Conclusions

[46] For the first time we explicitly model the iron produced during combustion: both from industrial and biomass burning sources. Industrial sources of iron are deduced based on literature values of the emission factors and a model of combustion sources globally [*Bond et al.*, 2004]. Emissions of iron from biomass burning is based on observed ratios of iron to black carbon in the Amazon and biomass burning estimates based on the combination of satellite observations of fires and terrestrial carbon models [*van der Werf et al.*, 2003]. These estimates suggest that as previously assumed, iron from mineral aerosols dominate the global average and most of the ocean deposition. However, far from dust regions and close to industrial regions or biomass burning regions, iron from combustion sources may be important.
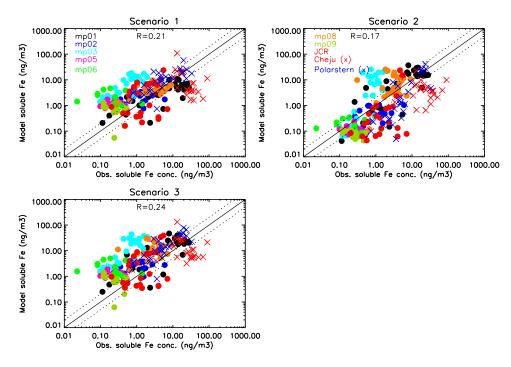
Figure 9. Comparisons of soluble iron concentrations for the cruises shown in Figure 2, for the scenarios 1 (SOLFE_COMB_AP + SOLFE_DUST_AP), 2 (SOLFE_COMB_BC + SOLFE_DUST_EM) and 3 (sum of scenario 1 and 2).

[47] Previously, most studies have assumed that soluble iron (presumably related to the bioavailable fraction) is from mineral aerosols [e.g., *Jickells and Spokes*, 2001; *Mahowald et al.*, 2005a, 2005b]. Because soil soluble iron fractions are so small, researchers proposed that atmospheric processing of iron was responsible for the larger downwind solubilities [*Zhu et al.*, 1992; *Jickells and Spokes*, 2001; *Hand et al.*, 2004; *Mahowald et al.*, 2006; *Luo et al.*, 2005; *Fan et al.*, 2006]. Observations at Cheju, Korea, which are much closer to combustion and dust sources than previous soluble iron measurements, are inconsistent with our modeling of soluble iron processing in the atmosphere. *Chuang et al.* [2005] suggested that these observations are most consistent with a combustion source of soluble iron. Here we test that assumption using a model that can simulate pollution transport and events at the observing stations. Only by assuming that soluble iron is not correlated with total iron emissions can our model simulations match the Cheju observations Instead, we assume that soluble iron (Fe(II)) emissions are related to black carbon emissions, perhaps because of incomplete combustion being important for emissions of both. Fe(III) is the insoluble and more oxidized alternative to Fe(II). The relationship between Fe(II) and BC assumed here is based on only 26 daily averaged measurements at Cheju, Korea, and thus should be improved in future studies.

[48] Assuming that soluble iron is emitted directly by combustion and that only a small amount of soluble iron is included in emitted dust (and no atmospheric processing takes place) implies that over most of the oceans, combustion sources of soluble iron dominate. Alternatively, one can assume that soluble iron is emitted directly and that atmospheric processing of total iron also takes place. In this case, combustion-soluble iron represents greater than 20% of the soluble iron deposition over much of the open oceans. The limited available observations cannot distinguish between these cases, while the observations at Cheju are not consistent with the atmospheric processing case alone.

[49] In addition to providing maps of soluble iron deposition which can be used in ocean biogeochemical models, this study has identified regions where combustion iron may be important. Some regions that are likely to be iron limited (e.g. eastern equatorial Pacific or the Southern Ocean which are far from dust sources) are especially regions where the inputs of soluble iron from combustion may be important. This implies that humans may already be perturbing the availability of iron in iron-limited regions by a large factor (Figure 10). Unfortunately, because of the loss of the core top during extraction of marine sediment cores, we do not have the ability to test whether there have been changes in dust deposition or productivity over the last century. One location where we do have some evidence for a shift in ecosystem response is at the Hawaii Ocean Time series [*Karl et al.*, 2001]. It is possible that shifts in the soluble iron amounts associated with industrial activity in Asia may be playing a role in changes in the ecosystem dynamics in the Pacific Ocean, although this region is not the most strongly impacted by combustion sources of iron according to our study.

[50] These results suggest that ignoring direct anthropogenic emissions of iron, as in previous studies, may result in substantial underestimates in the impact of humans on
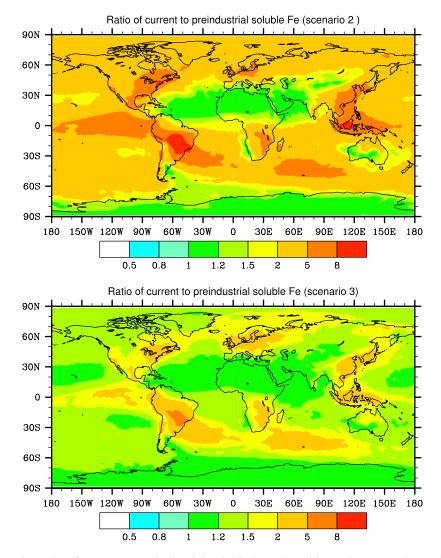
Figure 10. The ratio of current to preindustrial soluble iron deposition using scenario 2 (a) and 3 (b). We assume that preindustrial black carbon emissions and soluble iron emissions are 10% of current day.

atmospheric soluble or bioavailable iron, especially in HNLC regions. We consider this a first study modeling combustion iron and soluble iron; our main result is that more refined studies are justified to better understand the role of humans in modulating deposition of bioavailable iron.

References

Andreae, M. O., and P. Merlet (2001), Emission of trace gases and aerosols from biomass burning, *Global Biogeochem. Cycles*, *15*, 955–966.

Artaxo, P., and W. Maenhant (1990), Aerosol characteristics and sources for the Amazon basin during the west season, *J. Geophys. Res.*, *95*, 16,971–16,985.

Azuma, K., and H. Kametani (1964), Kinetics of dissolution of ferric oxide, *Trans. Metall. Soc. AIME*, *230*, 853–862.

Baker, A. R., and T. D. Jickells (2006), Mineral particle size as a control on aerosol iron solubility, *Geophys. Res. Lett.*, *33*, L17608, doi:10.1029/2006GL026557.

Baker, A. R., S. D. Kelly, K. F. Biswas, M. Witt, and T. D. Jickells (2003), Atmospheric deposition of nutrients to the Atlantic Ocean, *Geophys. Res. Lett.*, *30*(24), 2296, doi:10.1029/2003GL018518.

Baker, A., T. Jickells, K. Biswas, K. Weston, and M. French (2006), Nutrients in atmospheric aerosol particles along the Atlantic Meridional Transect, *Deep Sea Res. II*, *53*, 1706–1719.

Barth, M. C., P. J. Rasch, and J. T. Kiehl (2000), Sulfur chemistry in National Center for Atmospheric Research Community Climate Model: Description, evaluation features, and sensitivity to aqueous chemistry, *J. Geophys. Res.*, *105*, 1387–1415.

Benkoviz, C. M., M. T. Scholtz, J. Pacyna, L. Tarrason, J. Dignon, E. C. Voldner, P. A. Spiro, J. A. Logan, and T. E. Graedel (1996), Global gridded inventories of anthropogenic emissions of sulfur and nitrogen, *J. Geophys. Res.*, *101*, 29,239–29,254.

Blesa, M. A., P. J. Morando, and A. E. Regazzoni (1994), *Chemical Dissolution of Metal Oxides*, 401 pp., CRC Press, Boca Raton, Fla.

Bond, T. C., D. G. Streets, K. F. Yarber, S. M. Nelson, J.-H. Woo, and Z. Klimont (2004), A technology-based global inventory of black and organic carbon emissions from combustion, *J. Geophys. Res.*, *109*, D14203, doi:10.1029/2003JD003697.

Cama, J., C. Ayora, and A. C. Lasaga (1999), The deviation-from-equilibrium effect on dissolution rate and on apparent variations in activation energy, *Geochim. Cosmochim. Acta*, *63*(17), 2481–2486.

Capone, D. G., J. P. Zehr, H. W. Paerl, B. Bergman, and E. J. Arpenter (1997), Trichodesmium, a globally significant marine cyanobacterium, *Science*, *276*, 1221–1229.

Chen, M., R. C. H. Dei, W. X. Wang, and L. D. Guo (2003), Marine diatom uptake of iron bound with natural colloids of different origin, *Mar. Chem.*, *81*, 177–189.

Chen, Y. (2004), Sources and fate of atmospheric nutrients over the remote oceans and their role on controlling marine diazotrophic microorganisms, Ph.D. diss., Chesapeake Biol. Lab., Cent. for Environ. Sci., Univ. of Md., Solomons.

Chen, Y., and R. Siefert (2003), Determination of various types of labile atmospheric iron over remote oceans, *J. Geophys. Res.*, *108*(D24), 4774, doi:10.1029/2003JD003515.

Chen, Y., and R. Siefert (2004), Sesaonal and spatial distributions and dry deposition fluxes of atmospheric total and labile iron over the tropical and subtropical North Atlantic Ocean, *J. Geophys. Res.*, *109*, D09305, doi:10.1029/2003JD003958.

Chin, M., P. Ginoux, R. Lucchesi, B. Huebert, R. Weber, T. Anderson, S. Masonis, B. Blomquist, A. Bandy, and D. Thornton (2003), A global aerosol model forecast for the ACE-Asia field experiment, *J. Geophys. Res.*, *108*(D23), 8654, doi:10.1029/2003JD003642.

Chuang, P. Y., R. M. Duvall, M. M. Shafer, and J. J. Schauer (2005), The origin of water soluble particulate iron in the Asian atmospheric outflow, *Geophys. Res. Lett.*, *32*, L07813, doi:10.1029/2004GL021946.

Claquin, T., M. Schulz, and Y. Balkanski (1999), Modeling the mineralogy of atmospheric dust sources, *J. Geophys. Res.*, *104*, 22,243–22,256.

Collins, W. D., P. J. Rasch, B. E. Eaton, B. V. Khattatov, J.-F. Lamarque, and C. S. Zender (2001), Simulating aerosols using a chemical transport model with assimilation of satellite aerosol retrievals: Methodology of INDOEX, *J. Geophys. Res.*, *106*, 7313–7336.

Cornell, R. M., and U. Schwertmann (1996), *The Iron Oxides: Structure, Properties, Reactions, Occurrences and Uses*, 573 pp., John Wiley, Hoboken, N. J.

Duce, R. A., and N. W. Tindale (1991), Atmospheric transport of iron and its deposition in the ocean, *Limnol. Oceanogr.*, *36*(8), 1715–1726.

Falkowski, P. G., R. T. Barber, and V. Smetacek (1998), Biogeochemical controls and feedbacks on ocean primary production, *Science*, *281*, 200–206.

Fan, S.-M., W. J. Moxim, and H. Levy II (2006), Aeolian input of bioavailable iron to the ocean, *Geophys. Res. Lett.*, *33*, L07602, doi:10.1029/2005GL024852.

Flagan, R. C., and S. K. Friedlander (1978), Particle formation in pulverized coal combustion: A review, in *Recent Developments in Aerosol Science*, edited by D. T. Shaw, pp. 25–59, John Wiley, New York.

Fung, I., S. Meyn, I. Tegen, S. C. Doney, J. John, and J. K. B. Bishop (2000), Iron supply and demand in the upper ocean, *Global Biogeochem. Cycles*, *14*, 281–296.

Fuzzi, S., et al. (2007), Overview of the inorganic and organic composition of size-segregated aerosol in Rondônia, Brazil, from the biomass-burning period to the onset of the wet season, *J. Geophys. Res.*, *112*, D01201, doi:10.1029/2005JD006741.

Gaudichet, A., F. Echalar, B. Chatenet, J. P. Quisefit, G. Malingre, H. Cachier, P. Buat-Menard, P. Artaxo, and W. Maenhaut (1995), Trace elements in tropical African savanna biomass burning aerosols, *J. Atmos. Chem.*, *22*, 19–39.

Ginoux, P., M. Chin, I. Tegen, J. Prospero, B. Holben, O. Dubovik, and S. J. Lin (2001), Sources and distributions of dust aerosols simulated with the GOCART model, *J. Geophys. Res.*, *106*, 20,255–20,273.

Guieu, C., S. Bonnet, T. Wagener, and M.-D. Loye-Pilot (2005), Biomass burning as a source of dissolved iron to the open ocean?, *Geophys. Res. Lett.*, *22*, L19608, doi:10.1029/2005GL022962.

Hand, J. L., N. Mahowald, Y. Chen, R. Siefert, C. Luo, A. Subramaniam, and I. Fung (2004), Estimates of soluble iron from observations and a global mineral aerosol model: Biogeochemical implications, *J. Geophys. Res.*, *109*, D17205, doi:10.1029/2004JD004574.

Hildemann, L., G. Markowski, and G. Cass (1991), Chemical composition of emissions from urban sources of fine organic aerosol, *Environ. Sci. Technol.*, *25*, 744–759.

International Energy Agency (1998a), *Energy Statistics of OECD Countries*, Int. Energy Agency, Paris.

International Energy Agency (1998b), *Energy Statistics of Non-OECD Countries*, Int. Energy Agency, Paris.

Jickells, T. and L. Spokes (2001), Atmospheric iron inputs to the oceans, in *Biogeochemistry of Iron in Seawater*, *IUPAC Ser. on Anal. and Phys.*

Chem., vol. 7, edited by D. R. Turner and K. A. Hunter, pp. 85–121, John Wiley, Chichester.

Karl, D. M., K. M. Björkman, J. E. Dore, L. A. Fujieki, D. V. Hebel, T. Houlihan, R. M. Letelier, and L. M. Tupas (2001), Ecological nitrogen-to-phosphorus stoichiometry at station ALOHA, *Deep Sea Res., Part II*, *48*, 1449–1470.

Kistler, R., et al. (2001), The NCEP-NCAR 5-year reanalysis: Monthly means CD-ROM and documentation, *Bull. Am. Meteorol. Soc.*, *82*(2), 247–267.

Kleeman, M. J., J. J. Schauer, and G. R. Cass (2000), Size and composition distribution of fine particulate matter emitted from motor vehicles, *Environ. Sci. Technol.*, *34*(7), 1132–1142.

Lasaga, A. C., J. M. Soler, J. Ganor, T. E. Burch, and K. L. Nagy (1994), Chemical-weathering rate laws and global geochemical cycles, *Geochim. Cosmochim. Acta*, *58*(10), 2361–2386.

Lee, S., et al. (2005), Gaseous and particulate emissions from prescribed burning in Georgia, *Environ. Sci. Technol.*, *39*, 9049–9056.

Linak, W. P., C. A. Miller, and J. O. L. Wendt (2000), Comparison of the particle size distributions and elemental partitioning from the combustion of pulverized coal and residual fuel oil, *J. Air Waste Manage. Assoc.*, *50*, 1532–1544.

Luo, C., N. M. Mahowald, and J. del Corral (2003), Sensitivity study of meteorological parameters on mineral aerosol mobilization, transport, and distribution, *J. Geophys. Res.*, *108*(D15), 4447, doi:10.1029/2003JD003483.

Luo, C., N. M. Mahowald, N. Meskhidze, Y. Chen, R. L. Siefert, A. R. Baker, and A. M. Johansen (2005), Estimation of iron solubility from observations and a global aerosol model, *J. Geophys. Res.*, *110*, D23307, doi:10.1029/2005JD006059.

Mahowald, N. M., P. J. Rasch, B. E. Eaton, S. Whittleston, and R. G. Prinn (1997), Transport of 222 Radon to the remote troposphere using MATCH and assimilated winds from ECMWF and NCEP/NCAR, *J. Geophys. Res.*, *102*, 28,139–28,151.

Mahowald, N., C. S. Zender, C. Luo, D. Savoie, O. Torres, and J. del Corral (2002), Understanding the 30-year Barbados desert dust record, *J. Geophys. Res.*, *107*(D21), 4561, doi:10.1029/2002JD002097.

Mahowald, N., C. Luo, J. del Corral, and C. S. Zender (2003), Interannual variability in atmospheric mineral aerosols from a 22-year model simulation and observational data, *J. Geophys. Res.*, *108*(D12), 4352, doi:10.1029/2002JD002821.

Mahowald, N. M., A. R. Baker, G. Bergametti, N. Brooks, R. A. Duce, T. D. Jickells, N. Kubilay, J. M. Prospero, and I. Tegen (2005a), Atmospheric global dust cycle and iron inputs to the ocean, *Global Biogeochem. Cycles*, *19*, GB4025, doi:10.1029/2004GB002402.

Mahowald, N. M., P. Artaxo, A. R. Baker, T. D. Jickells, G. S. Okin, J. T. Randerson, and A. R. Townsend (2005b), Impacts of biomass burning emissions and land use change on Amazonian atmospheric phosphorus cycling and deposition, *Global Biogeochem. Cycles*, *19*, GB4030, doi:10.1029/2005GB002541.

Mahowald, N. M., D. R. Muhs, S. Levis, P. J. Rasch, M. Yoshioka, C. S. Zender, and C. Luo (2006), Change in atmospheric mineral aerosols in response to climate: Last glacial period, preindustrial, modern, and doubled carbon dioxide climates, *J. Geophys. Res.*, *111*, D10202, doi:10.1029/2005JD006653.

Mamane, Y., J. Miller, and T. Dzubay (1986), Characterization of individual fly ash particles emitted from coal- and oil-fired power plants, *Atmos. Environ.*, *20*, 2125–2135.

Mamuro, T., A. Mizohata, and T. Kubota (1979a), Elemental compositions of suspended particles released from iron and steel works, *Annu. Rep. Radiat. Cent. Osaka Prefecture*, *20*, 19–28.

Mamuro, T., A. Mizohata, and T. Kubota (1979b), Elemental compositions of suspended particles released from various small sources (II), *Annu. Rep. Radiat. Cent. Osaka Prefecture*, *20*, 47–53.

Martin, J. H., R. M. Gordon, and S. E. Fitzwater (1991), The case for iron, *Limnol. Oceanogr.*, *36*, 1793–1802.

McElroy, M. W., R. C. Carr, D. S. Ensor, and G. R. Markowski (1981), Size distribution of fine particles from coal combustion, *Science*, *215*, 13–19.

Meskhidze, N., W. L. Chameides, A. Nenes, and G. Chen (2003), Iron mobilization in mineral dust: Can anthropogenic SO2 emissions affect ocean productivity?, *Geophys. Res. Lett.*, *30*(21), 2085, doi:10.1029/2003GL018035.

Nishioka, J., S. Takeda, H. J. W. de Baar, P. L. Coot, M. Boye, P. Laan, and K. R. Timmermans (2005), Changes in concentrations if iron in different size fractions during an iron enrichment experiment in the open Southern Ocean, *Mar. Chem.*, *95*, 51–63.

Novakov, T., D. A. Hegg, and P. V. Hobbs (1997), Airborne measurements of carbonaceous aerosols on the East coast of the United States, *J. Geophys. Res.*, *102*, 30,023–30,030.

Olmez, I., A. Sheffield, G. Gordon, J. Houck, L. Pritchett, J. Cooper, T. G. Dzubay, and R. Bennett (1988), Compositions of particles from selected sources in Philadelphia for receptor modeling applications, *J. Air Pollut. Control Assoc.*, *38*, 1392–1402.

Parekh, P., M. J. Follows, and E. Boyle (2004), Modeling the global ocean iron cycle, *Global Biogeochem. Cycles*, *18*, GB1002, doi:10.1029/2003GB002061.

Rasch, P. J., N. M. Mahowald, and B. E. Eaton (1997), Representation of transport, convection and hydrologic cycle in chemical transport models: Implications for the modeling of short-lived and soluble species, *J. Geophys. Res.*, *102*, 18,127–18,138.

Rasch, P. J., M. C. Barth, J. T. Kiehl, S. E. Schwartz, and C. M. Benkovitz (2000), A description of the global sulfur cycle and its controlling processes in the National Center for Atmospheric Research Community Climate Model, Version 3, *J. Geophys. Res.*, *105*, 1367–1385.

Rasch, P. J., W. D. Collins, and B. E. Eaton (2001), Understanding the Indian Ocean Experiment (INDOEX) aerosol distributions with an aerosol assimilation, *J. Geophys. Res.*, *106*, 7337–7355.

Saydam, A. C., and H. Z. Senyuva (2002), Deserts: Can they be the potential supplies of bioavailable iron?, *Geophys. Res. Lett.*, *29*(11), 1524, doi:10.1029/2001GL013562.

Sedwick, P. N., E. R. Sholkovitz, and T. M. Church (2007), Impact of anthropogenic combustion emissions on the fractional solubility of aerosol iron: Evidence from the Sargasso Sea, *Geochem. Geophys. Geosyst.*, *8*, Q10Q06, doi:10.1029/2007GC001586.

Seinfeld, J., and S. Pandis (1996), *Atmospheric Chemistry and Physics: From Air Pollution to Climate Change*, John Wiley, New York.

Siefert, R. L., A. M. Johansen, M. R. Hofmann, and S. O. Pehkonen (1997), Measurements of trace metal (Fe, Cu, Mn, Cr) oxidation states in fog and stratus clouds, *J. Air Waste Mange. Assoc.*, *48*, 128–143.

Skopp, J. M. (2000), Physical properties of primary particles, in *Handbook of Soil Science*, edited by M. E. Summer, pp. 3–17, CRC Press, Boca Raton, Fla.

Smith, R., J. Campbell, and K. Nielson (1979), Characterization and formation of submicron particles in coal-fired plants, *Atmos. Environ.*, *13*, 607–617.

van der Werf, G. R. V. D., J. T. Randerson, G. J. Collatz, and L. Gilio (2003), Carbon emissions from fires in tropical and subtropical ecosystems, *Global Change Biol.*, *9*, 547–562.

Willey, J., et al. (2004), Effects of rainwater iron and hydrogen peroxide on iron speciation and phytoplankton growth in sea water near Bermuda, *J. Atmos. Chem.*, *47*, 209–222.

Yamasoe, M., P. Artaxo, A. Miguel, and A. Allen (2000), Chemical composition of aerosol particles from direct emissions of vegetation fires in the Amazon Basin: Water-soluble species and trace elements, *Atmos. Environ.*, *34*, 1641–1653.

Zender, C. S., H. Bian, and D. Newman (2003), Mineral Dust Entrainment and Deposition (DEAD) model: Description and 1990s dust climatology, *J. Geophys. Res.*, *108*(D14), 4416, doi:10.1029/2002JD002775.

Zhu, X., J. M. Prospero, F. J. Millero, D. L. Savoie, and G. W. Brass (1992), The solubility of ferric iron in marine mineral aerosol solution at ambient relative humidities, *Mar. Chem.*, *38*, 91–107.

Zhu, X., J. M. Prospero, and F. J. Millero (1997), Diel variability of soluble Fe(II) and soluble total Fe in North African dust in the trade winds at Barbados, *J. Geophys. Res.*, *102*, 21,297–21,305.

Zhuang, G., Z. Yi, R. A. Duce, and P. R. Brown (1992), Link between iron and sulphur cycles suggested by detection of Fe(II) in remote marine aerosols, *Nature*, *355*, 537–539.

Zinder, B., G. Furrer, and W. Stumm (1986), The coordination chemistry of weathering: II. Dissolution of Fe(III) oxides, *Geochim. Cosmochim. Acta*, *50*(9), 1861–1869.

Zuo, Y., and J. Hoigné (1992), Formation of hydrogen peroxide and depletion of oxalic acid in atmospheric water by photolysis of iron (III)-oxalato complexes, *Environ. Sci. Technol.*, *26*, 1014–1022.

———————————

P. Artaxo, Instituto de Fisica, Universidade de Sao Paulo, Caixa Postal 66318, CEP 05315-970, Sao Paolo, Brazil. (artaxo@if.usp.br)

T. Bond, Department of Civil and Environmental Engineering, University of Illinois at Urbana-Champaign, NCEL, M-250, 205 North Mathews Avenue, Urbana, IL 61801, USA. (yark@uiuc.edu)

Y. Chen, Department of Geological and Environmental Sciences, Stanford University, Stanford, CA 94305, USA. (yingcheny@yahoo.com)

P. Y. Chuang, Department of Earth Science, University of California, Santa Cruz, 1156 High Street, Santa Cruz, CA 95064, USA. (pchuang@es.ucsc.edu)

C. Luo, Department of Earth System Science, University of California, Irvine, CA 92717, USA. (cluo@uci.edu)

N. Mahowald, Department of Earth and Atmospheric Sciences, Cornell University, 2140 Snee Hall, Cornell, NY 14853, USA.

J. Schauer, Department of Civil and Environmental Engineering, University of Wisconsin-Madison, 660 North Park Street, Madison, WI 53706, USA. (jjschauer@wisc.edu)

R. Siefert, Chemistry Department, U.S. Naval Academy, 572M Holloway Road, Annapolis, MD 21402, USA. (siefert@usna.edu)